Arg-14 Loop of Site 3 Anemone Toxins: Effects of Glycine Replacement on Toxin Affinity[†,‡]

Anna L. Seibert,[§] Jinrong Liu,[||] Dorothy A. Hanck,[||] and Kenneth M. Blumenthal*[,§]

Department of Biochemistry, State University of New York at Buffalo, Buffalo, New York 14214, and Departments of Medicine and Pharmacological and Physiological Sciences, University of Chicago, Chicago, Illinois 60637

Received July 22, 2003; Revised Manuscript Received October 7, 2003

ABSTRACT: Anthopleurin B (ApB) is a high-affinity sea anemone neurotoxin that interacts with voltage-sensitive sodium (Na_V) channels, causing a delay in channel inactivation. The solution structures of all known anemone toxins having this activity include a poorly defined region encompassing ApB residues 8−17, which we call the Arg-14 loop. We propose that the inherent mobility of the Arg-14 loop is necessary for the toxins' ability to maintain a high-affinity channel complex throughout the continual conformational transitions experienced by the channel during its functional cycle. We have previously shown that Arg-12, located in this loop, and Leu-18, which is adjacent, are important for ApB activity. Here, we characterized the role of two glycines located within the loop (Gly-10 and Gly-15) and an additional glycine positioned immediately C-terminal to it (Gly-20). We used site-directed replacement by alanine to assess the functional contribution to toxin binding of each of these residues singly and in combination. Gly-20 was found to be an essential toxin folding determinant; Gly-10 and Gly-15 were important for determining toxin affinity. Compared to wild-type toxin, the G10A and G15A toxins displayed significantly higher K_D values for both cardiac ($Na_V1.5$) and neuronal ($Na_V1.2$) channels, although both demonstrated greater isoform discrimination for $Na_V1.5$ than did wild-type ApB. For both G10A and G15A, significant Na_V isoform differences were evident for on- and off-rates, with the most dramatic effect of a single mutation being the 467-fold reduction in the on-rate for G10A binding to $Na_V1.2$, suggestive of a more accommodating binding site on $Na_V1.5$ as compared to $Na_V1.2$. Because alanine replacement of glycines is known to be associated with reduced backbone freedom, these results suggest an essential role for Arg-14 loop flexibility in toxin function, although a direct steric effect of the mutant methyl group cannot be excluded.

Many toxins are known to interact with voltage-sensitive sodium channels (Na_V's)[1] at distinct binding sites (*1*−*4*), causing either channel blockage or alterations in activation or inactivation kinetics. Upon membrane depolarization, Na_V channels undergo conformational changes from the resting to the activated state, followed immediately by a transition to the inactivated state. Binding of the structurally unrelated anemone and α-scorpion toxins to site 3 delays inactivation by inhibiting this last conformational transition (*5*−*10*).

Anthopleurin B (ApB) is a type I sea anemone toxin (*8*) isolated from *Anthopleura xanthogrammica*, which binds to site 3 of Na_V channels. ApB is a 49-residue polypeptide neurotoxin cross-linked by three disulfide bonds in a conformation that is primarily a β-structure. The solution structure of ApB, like all type I sea anemone toxins, contains a four-stranded antiparallel β-sheet (residues 2−4, 20−23, 34−37, and 45−48) linked by β-turns and loops with no α-helix (Figure 1; *10*−*12*; PDB code 1apf). While the three conserved disulfide bonds Cys4−Cys46, Cys6−Cys36, and Cys29−Cys47) of type I anemone toxins provide a rigid core for the polypeptide, one region called the Arg-14 loop (ApB residues 8−17; *10*, *13*) displays a high degree of disorder. All known type I anemone toxin structures reveal few medium- and long-range constraints for these residues. Nonetheless, conservation of this loop in all known site 3 anemone toxins suggests that it plays an important functional role.

Using the recombinant system developed in our laboratory (*14*), we have previously demonstrated that two residues, Arg-12 and Leu-18, located within and adjacent to the Arg-14 loop, respectively, are important for ApB channel affinity as well as cardiac ($Na_V1.5$) vs neuronal ($Na_V1.2$) isoform selectivity (*15*−*17*). These results suggest that at least a portion of the Arg-14 loop region is in contact with Na_V channels. Further work from our laboratories using mutant cycle analysis demonstrated that Lys-37 of ApB interacts with Asp-1612 located in the S3−S4 loop of DIV of rat $Na_V1.5$ (*18*). This residue is homologous to Glu-1613 of rat $Na_V1.2$, which has been shown to interact with the site 3 α-scorpion toxin LqTx and the anemone toxin ATX II (*19*).

[†]This work was supported by Grants GM-60582 (to K.M.B. and D.A.H.) from the National Institutes of Health and AHA0110113T (to A.L.S.) from the American Heart Association.

[‡] Portions of this work have been presented in abstract format in *Biophys. J.*, 2003.

* To whom correspondence should be addressed. E-mail: kblumen@buffalo.edu. Phone: (716) 829-2727. Fax: (716) 829-2725.

[§] State University of New York at Buffalo.

[||] University of Chicago.

[1] Abbreviations: wt-ApB, wild-type anthopleurin B; ApA, anthopleurin A; Na_V, voltage-sensitive sodium channel.

10.1021/bi035291d CCC: $25.00
Published on Web 11/21/2003

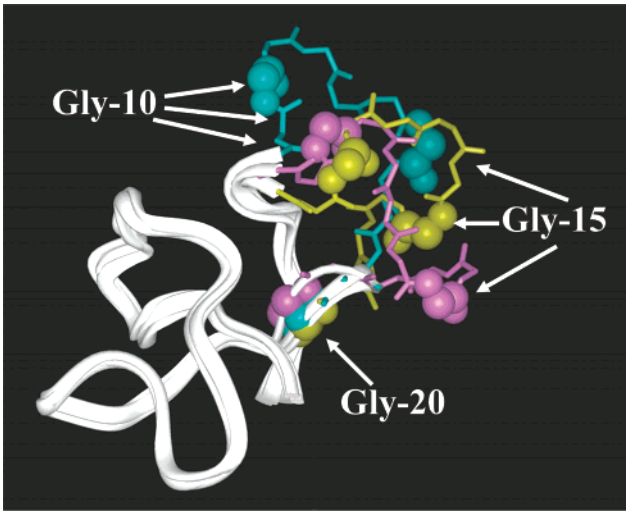

FIGURE 1: ApB Arg-14 loop flexibility. The three ApB structures shown (PDB code 1apf7, -2, and -15; *12*) represent the ensemble average (1apf7) and the most extreme displacements of the Arg-14 loop of ApB. The well-defined regions of the protein (residues 1−7 and 18−49) are represented by white backbone ribbons. The poorly defined Arg-14 loop region (residues 8−17) and the adjacent residues 18−20 are depicted in stick format, with Gly-10, Gly-15, and Gly-20 in space-filling mode. The average 1apf7 loop is colored yellow, while 1apf15 is pink and 1apf2 is blue. Notice the large variability in the positioning of Gly-10 and Gly-15, while Gly-20 is more closely overlaid in the three structures.

Aside from this single interaction, the biochemical nature of site 3 is not well understood. Additional characterization of this site could provide important insights into its ability to bind structurally diverse toxins with high affinity.

We were led to consider whether Arg-14 loop mobility per se contributes to the high affinity and isoform selectivity displayed by sea anemone toxins in general, and ApB in particular. Because glycines are unique in lacking a side chain, they confer greater conformational freedom upon their peptide backbone than does any other amino acid. Therefore, we proposed that the two glycine residues located within this loop (Gly-10 and Gly-15) and an additional glycine located just beyond the C-terminus of the loop (Gly-20) could contribute to its conformational mobility and ApB's affinity for Na_V channels. The work described here focuses on the replacement of these glycines by alanine individually and in combination, to determine their importance to the toxin's ability to modify gating kinetics of Na_V channels.

MATERIALS AND METHODS

Reagents and Enzymes. The highest grades of commercially available enzymes and chemicals were used for all experiments. General chemicals were purchased from Sigma-Aldrich (St. Louis, MO), while staphylococcal V8 protease was purchased from ICN (Costa Mesa, CA). Cell culture products, restriction enzymes, and IPTG were purchased from Invitrogen Life Technologies, Inc. (Carlsbad, CA).

Cell Culture. To analyze the effects of ApB on the human cardiac voltage-sensitive sodium channel, cDNA encoding human $Na_V1.5$ was cloned into plasmid $pRcCMV_{II}$ and stable cell lines were constructed in HEK-293 cells using neomycin selection. These cells were grown in low-glucose DMEM supplemented with 10% FBS, 1% penicillin−streptomycin, and 200 μg/mL G418 in 5% CO_2. The murine neuroblastoma cell line N1E-115 was obtained from ATCC (Manassas, VA) and used to study the effects of ApB on neuronal sodium channels. Because N1E-115 cells primarily express $Na_V1.2$ (*20*), we ascribe ApB binding detected in this cell line to this isoform. It should be noted, however, that low-level expression of $Na_V1.3$ and -1.7 has also been detected in these cells (*21*). N1E-115 cells were grown in high-glucose DMEM supplemented with 10% FBS and 1% penicillin−streptomycin in 5% CO_2. To prepare both cell lines for study, they were trypsinized, centrifuged, and resuspended in media and then either placed on coverslips and returned to the incubator for use later that day or placed directly in the cell chamber for use at that time.

Molecular Biology. Site-directed mutagenesis was performed using the QuikChange system (Stratagene, La Jolla, CA) in the recombinant plasmid pKB13 previously described by our laboratory (*14*) or in the pKB13-derived plasmid pJL2. pJL2 is identical to pKB13 except that the sequence encoding the pentaglutamyl linker fusing ApB to the C-terminal end of the bacteriophage T7 gene 9 protein was changed to encode KGEEM. Nucleotide sequences of all derived plasmids were validated by the dideoxy method to ensure that the correct product was produced. All variant proteins will be referred to by the single-letter abbreviation of the wt-ApB amino acid followed by its position number and the single-letter abbreviation for the replacement amino acid. The mutagenesis yielded the plasmids pAS20 (G10A), pAS17 (G15A), pAS18 (G20A), pAS27 (G10A/G15A), pAS23 (G10A/G20A), and pAS19 (G15A/G20A).

Protein Purification and Analytical Methods. ApB and all variants were expressed in *Escherichia coli* BL21(DE3) as fusion proteins under the control of the T7 promoter. Following purification of the fusion protein by anion exchange chromatography, disulfide pairs were oxidized using a glutathione redox couple, and then ApB was released by hydrolysis with V8 protease, followed by final purification to homogeneity by reversed-phase HPLC on a C4 column (*14*). Molecular weights of purified toxins were then confirmed by MALDI-TOF MS (matrix-assisted laser desorption ionization time-of-flight mass spectrometry) analysis on a Bruker (Billerica, MA) Biflex IV spectrometer. For some pKB13-derived proteins, a second polypeptide having a single glutamyl N-terminal extension was also present. Cleavage of pJL2-derived proteins with V8 protease yields a form of ApB having an additional methionine residue at its amino terminus. We have previously shown that the glutamyl extension has no effect on toxin affinity (*22*), nor does a two-residue Gly−Arg extension (*14*). Therefore, mixtures of the 49- and 50-residue products were used without additional fractionation. Although the recovery for wild-type ApB is typically about 1−2 mg/4 L of culture, the yield of the G20A protein was much lower. We believe this decreased yield reflects the inability of G20A to fold to the active conformation with correct disulfide pairings. In contrast, the G10A, G15A, and G10A/G15A proteins were recovered at levels equivalent to that of wild-type toxin.

Secondary structural contents were determined by far-UV/circular dichroism (CD) spectropolarimetery on a Jasco (Easton, MD) J-710 spectropolarimeter. For CD analysis, all proteins were prepared at 20 μM in 5 mM sodium phosphate buffer, pH 6.9. Spectra were recorded at 0.1 nm increments

at a rate of 50 nm/min. The averages of four repeated spectra were smoothed and baseline subtracted. The folding status of mutant peptides was assessed by comparing their molecular ellipticities to that of wild-type toxin.

Electrophysiology. All toxin activities were measured by whole cell voltage clamp using an Axopatch 200B amplifier, a Digidata 1301 analogue converter, and the Clampex 8.1 software available from Axon Instruments (Union City, CA) running on a Pentium-based IBM-compatible computer. Data were filtered at 5 kHz. Borosilicate glass pipets were pulled and polished to 2−4 MΩ resistances. The bath solution used for N1E-115 cells was composed of 70 mM NaCl, 70 mM CsCl, 2 mM $CaCl_2$, and 10 mM Hepes, pH 7.4, titrated with CsOH. The bath solution for HEK-293 cells stably transfected with $Na_V1.5$ was the same except that the NaCl concentration was decreased to 2−10 mM and the CsCl concentration was increased accordingly to decrease the current magnitude and thereby maintain voltage control (*17*). The pipet solution for N1E-115 cells contained 90 mM CsF, 10 mM NaCl, 30 mM CsCl, 10 mM Hepes, and 10 mM EGTA, pH 7.0, titrated with CsOH. For the transfected HEK cells, the NaCl concentration was decreased to 2−5 mM and the CsF concentration was increased accordingly so that the internal:external sodium ratio maintained the reversal potential for sodium. Either suction or an electrical pulse was used on cells having gigaohm seal resistances to obtain whole cell access. All experiments were conducted at room temperature (22 °C).

Molecular Modeling. All designed mutant proteins were first modeled into the averaged ApB structure (*10*; PDB code 1apf) using the Insight and Discover programs (Accelrys, San Diego, CA) to assess the potential for steric hindrance due to replacement of glycine by alanine.

RESULTS

Molecular Modeling of Mutant ApB Proteins. All three proposed glycine to alanine substitutions were first generated in silico in the averaged solution structure of ApB (*10*) to assess the potential for induction of folding alterations. Mutant structures were then energy-minimized using a combined steepest descents and conjugate gradients protocol run in Discover. All substitutions generated models having energies and RMS differences comparable to those of the wt-ApB structure. Because no obvious mutationally induced structural conflicts were predicted, we proceeded to express and characterize the G10A, G15A, G10A/G15A, G20A, and G10A/G20A toxins.

Structural Characterization of ApB Mutant Proteins. To assess their secondary structures, the CD spectra of the mutant proteins G10A, G15A, G10A/G15A, G20A, and G10A/G20A were compared to that of wt-ApB (Figure 2). Similar to those of many polypeptide neurotoxins, these spectra were dominated by a large negative ellipticity in the vicinity of 200 nm (*23*, *24*). While the spectra of G10A, G15A, and G10A/G15A were essentially identical with that of wt-ApB, the spectrum of G20A had noticeable differences. This spectrum lacked the positive molecular ellipticity seen with wt-ApB around 230 and 190 nm, and the region from 212 to 222 nm lacked much of the characteristic shoulder due to the β-sheet content. The changes in the spectrum were even more pronounced in the double mutant G10A/G20A

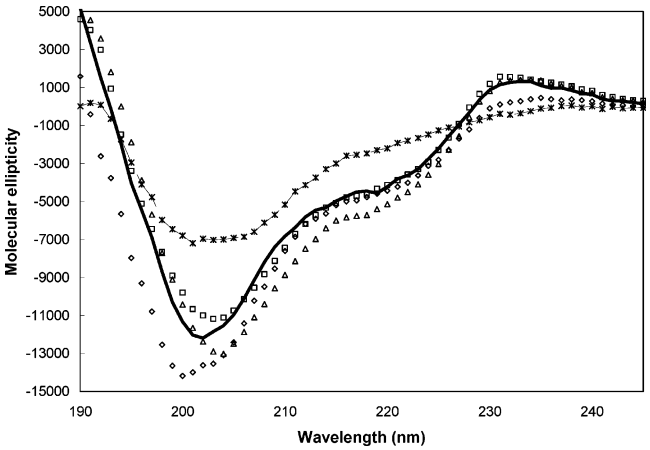

FIGURE 2: CD spectra of wt-ApB and mutant proteins. The molecular ellipticities for G10A (□), G15A (△), and G10A/G15A (◇) are similar to that of wt-ApB (solid line), while the spectrum for G20A (dashed line with asterisks) lacks the characteristic positive ellipticities at 190 and 235 nm, which are indicative of a folded structure.

(data not shown). On the basis of the altered CD spectra and routinely poor recoveries of mutant proteins containing G20A, we concluded that Gly-20 was an important folding determinant for ApB and performed no further characterization of these proteins.

Functional Characterization by Whole Cell Voltage Clamp. Whole cell voltage clamp analysis was used to measure the affinities of wt-ApB, G10A, G15A, and G10A/G15A for the $Na_V1.2$ and $Na_V1.5$ channels. The stable HEK cell line expressing human $Na_V1.5$ was prepared as described in the Materials and Methods. Individual cells were clamped to a voltage sufficiently negative (−130 mV) to ensure complete availability of Na_V channels upon membrane depolarization. Voltage control was determined by examination of the slope factor of the conductance transform, such that if this relationship was less than 4.7 mV/e-fold change, then the data were rejected. Only cells with greater than 0.5 GΩ seal resistances were accepted. A simple step protocol was used to measure time courses for modification and unmodification. Cells were perfused with either toxin-containing or toxin-free solution until full modification or unmodification, respectively, was achieved. Toxin concentrations ranged from 100 nM to 2 μM, depending on the affinity of the mutant toxin being analyzed. HEK-293 cells transfected with $Na_V1.5$ were stimulated for 11 ms by stepping the voltage to −30 mV, while N1E cells were stepped to −10 mV because these channels activate at more positive voltages. The frequency of stimulation varied between 0.1 and 1 Hz depending on the rate of modification or dissociation. Data were leak and capacitance corrected using a locally written Matlab (Natick, MA) program (*18*), and residual currents at 7−8 ms after depolarization were averaged (Figure 3A). This late current window average was normalized to the peak current of the control for modification analysis and to the maximal residual current at 7−8 ms for dissociation analysis, with the baseline residual current at 7−8 ms subtracted. The current at this late time window was used because channels not modified by ApB fully decay by this time; thus, the measured current was directly proportional to the number of modified channels in the cell. Currents were plotted vs time from initial toxin wash in or wash out. The data were fit to an exponential

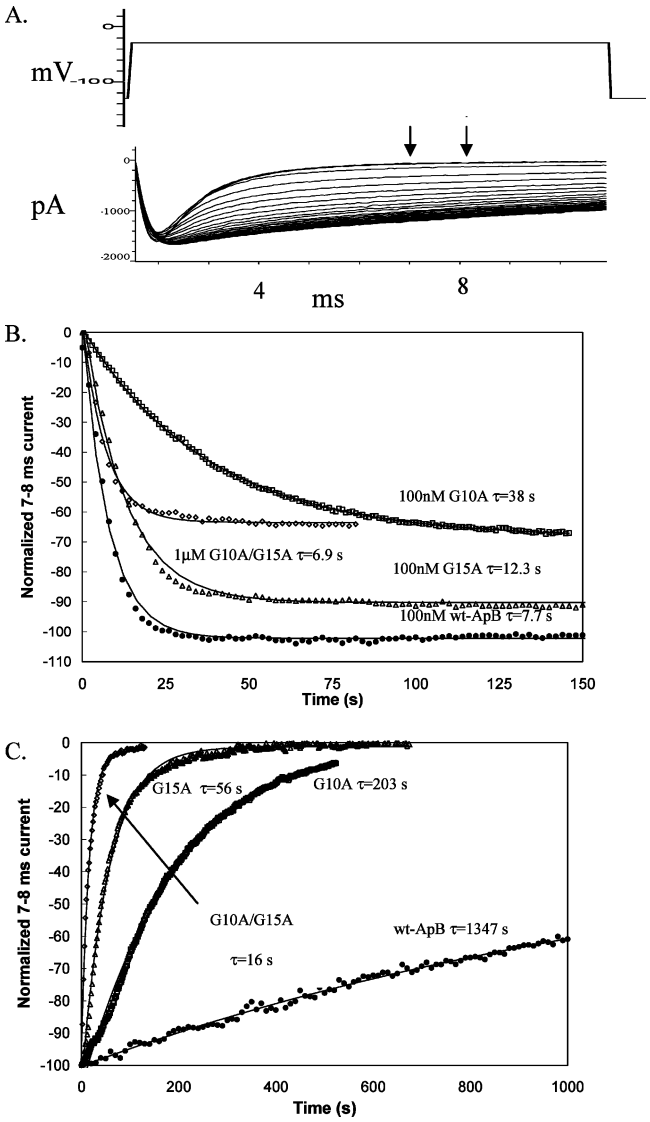

FIGURE 3: Modification and dissociation kinetics for $Na_V1.5$. A representative data set with the voltage step protocol used for $Na_V1.5$ is shown in (A). The arrows mark the 7−8 ms window current used to generate the modification (B) and dissociation (C) curves. Representative data for wt-ApB (●), G10A (□), G15A (△), and G10A/G15A (◇) are shown with overlaid fits. Data are normalized to the peak current as described in the text. A 100 nM concentration of toxin was used for wt-ApB, G15A, and G10A, while 1 μM was used for G10A/G15A.

function with a least-squares minimization routine with the software program Origin 6.1 (Microcal Software, Inc., Northampton, MA), where the inverse of the τ of the fit equals the kinetic constant for channel modification (k_{mod}) or the kinetic constant for the rate of toxin dissociation (k_{off}). From these association rate constants, a concentration-independent rate of toxin association was calculated using the equation $k_{on} = (k_{mod} - k_{off})/[\text{toxin}]$. The dissociation constant was then calculated from the averages of 3−12 cells using the association and dissociation constants in the equation $K_D = k_{off}/k_{on}$ (*18*).

Modification kinetics are concentration-dependent and therefore not directly comparable. However, concentration-independent association rates, calculated as described above, did allow such comparison. For $Na_V1.5$, the k_{on} for G10A was decreased slightly compared to that of wt-ApB, although the association rate of G15A was unchanged (Table 1). More

Table 1: Kinetic Constants for ApB and Mutant Proteins[a]

toxin	k_{on} ($10^5\ M^{-1}\ s^{-1}$)	k_{off} ($10^{-3}\ s^{-1}$)	K_D (nM)	DI
		$Na_V1.5$		
wt-ApB	10.9 ± 0.9 ($n = 12$)	1.29 ± 0.27 ($n = 8$)	1.2	
G10A	3.3 ± 0.7 ($n = 9$)	5.8 ± 1 ($n = 5$)	18	
G15A	10.2 ± 2.0 ($n = 6$)	15.7 ± 2.5 ($n = 6$)	15	
G10A/G15A	0.9 ± 0.09 ($n = 6$)	64.3 ± 9.2 ($n = 6$)	714	
		$Na_V1.2$		
ApB	22.5 ± 6.1 ($n = 8$)	12 ± 1.7 ($n = 6$)	5	4
G10A	0.049 ± 0.022 ($n = 3$)	11.4 ± 3.2 ($n = 3$)	2327	132
G15A	0.39 ± 0.06 ($n = 5$)	120 ± 20 ($n = 4$)	3077	200

[a] Kinetic constants were measured as described in the text. Averages are shown with standard errors. For k_{on}, if both k_{mod} and k_{off} were not available for one cell, the average value for the appropriate constant was used for the calculation. K_D values were calculated using the averaged values for k_{off} and k_{on}.

importantly, both toxins displayed 5−10-fold increases in dissociation rates (Table 1). When both substitutions were combined in G10A/G15A, a 50-fold increase in dissociation rate and a 12-fold decrease in association rate resulted. The decrease in association is ascribed to the G10A substitution, while the increased off-rate results from the combined effects of both replacements. These differences yield 15-, 13-, and 600-fold reductions in equilibrium dissociation constants for G10A, G15A, and G10A/G15A, respectively, compared to wild-type toxin.

In the present study, it is assumed that the kinetics of current modification is identical with the kinetics of toxin binding. In fact, wt-ApB and G15A were able to modify the 7−8 ms current window of $Na_V1.5$ to nearly 100% of the peak current (Figure 3B, Table 2), suggesting that toxin was bound to nearly all available channels. Conversely, the mutant toxins G10A and G10A/G15A did not fully modify all available channels on the basis of this assumption. When modification is less than 100%, the Langmuir adsorption isotherm can be applied to calculate K_D in an independent fashion. The K_D values calculated from kinetic measurements for all mutant toxins are in excellent agreement with those obtained using the Langmuir treatment (Table 2) with the exception of the binding of ApB to $Na_V1.2$, where affinity is thermodynamically underpredicted due to biphasic modification kinetics (see below). Therefore, we conclude that the incomplete modification of the 7−8 ms current found with G10A and G10A/G15A (Figure 3B) was due to the low affinity of these toxins.

Rates and constants were also measured in the same manner for the neuronal $Na_V1.2$ channel expressed in the neuroblastoma cell line N1E-115 (Figure 4, Table 1). Because the effects of combining G10A and G15A were additive when measured on $Na_V1.5$ channels, and because a large amount of protein would have been required to measure affinities to $Na_V1.2$ channels, further characterization of the doubly mutated toxin was not pursued. The effects of alanine substitution individually at Gly-10 and Gly-15 on $Na_V1.2$ channel modification were both qualitatively and quantitatively distinct from those observed with $Na_V1.5$ (Table 1). In this case, the decreases in channel affinities were largely due to decreases in the on-rates for both mutant toxins, with G10A toxin associating approximately 450-fold and G15A approximately 60-fold more slowly than did the wild type

Table 2: Extents of Modification for wt-ApB and Mutant Toxins[a]

toxin	extent of modification (%)	K_D (nM)	toxin	extent of modification (%)	K_D (nM)
			$Na_V1.5$		
wt-ApB ($n = 8$)	95 ± 5	5.3	G15A ($n = 6$)	90 ± 7	10
G10A ($n = 12$)	73 ± 7	37	G10A/G15A ($n = 6$)	69 ± 6	449
			$Na_V1.2$		
wt-ApB ($n = 5$)	58 ± 7	72	G15A ($n = 4$)	51 ± 7	1920
G10A ($n = 3$)	36 ± 4	3560			

[a] The extents of modification were calculated from cells to which the highest concentration of a given toxin was applied. Once toxin saturation was achieved, the current at 7−8 ms after depolarization was measured and is reported as a percentage of the peak current before toxin addition. Averages of 3−12 cells are given with standard errors. K_D values were calculated from the average extent of modification using the Langmuir equation $K_D = C(1/f_{mod} - 1)$ and are in close agreement with the K_D values reported in Table 1 with the exception of wt-ApB binding to $Na_V1.2$ (see comments in the text).

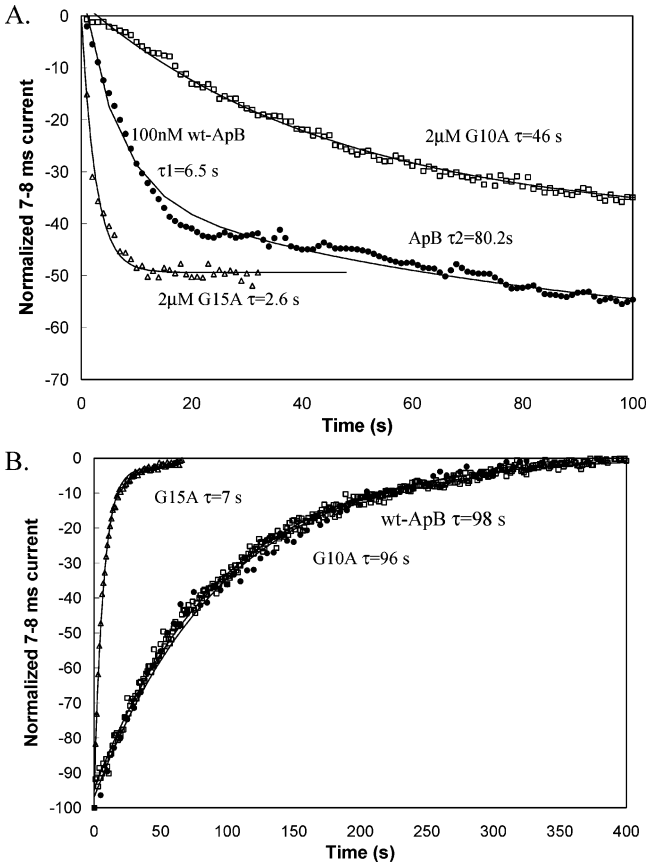

FIGURE 4: Modification and dissociation kinetics for $Na_V1.2$. Representative data are shown with overlaid fits as follows: wt-ApB (●), G10A (□), G15A (△). Data are normalized as described in the text. A 100 nM toxin concentration was used for wt-ApB, while 2 μM was used for G10A and G15A.

(Table 1). In contrast to our results with $Na_V1.5$, only the G15A mutation exhibited an increased rate of toxin dissociation from $Na_V1.2$. These isoform-specific on- and off-rate effects imply the existence of fundamental differences in the nature of the $Na_V1.5$ and $Na_V1.2$ sites 3 (Table 1).

The extent of rapid modification of $Na_V1.2$ by wt-ApB, G10A, and G15A was approximately 50% of the peak current. However, higher concentrations of wt-ApB were able to modify this channel to nearly 100% (data not shown). The Langmuir equation predicted K_D values comparable to those derived kinetically (Table 2) for G10A and G15A toxins, consistent with the assumption that toxin binding is equivalent to current modification. However, the kinetic and thermodynamic estimates of K_D do not agree as well in the case of wt-ApB. We feel that the kinetic estimates are more accurate, especially since inspection of the kinetics of modification of $Na_V1.2$ by wt-ApB reveals this process to be biphasic, with a slow second phase having an average time constant of 3 min. Because 58% of the modification is accounted for by the faster phase, its τ value was used to calculate the toxin on-rate. However, it is likely that the existence of the slower component compromises our ability to accurately gauge the extent of modification by wild-type toxin, thereby leading us to underestimate its affinity using the Langmuir treatment. In fact, when the *total* extent of modification is used to estimate K_D, the resulting value (17 nM) is in good agreement with kinetic measurements. It is intriguing that in very recent experiments we have seen hints of such biphasic association kinetics in the analysis of other mutant toxins (data not shown).

The changes we observed in binding kinetics for the mutant toxins resulted in significantly altered isoform selectivity. We have previously defined the term discrimination index (DI) as being the ratio of $K_{D(Na_V1.2)}/K_{D(Na_V1.5)}$ for a given toxin. Wild-type ApB displayed a DI of approximately 4. In contrast, despite their much lower overall affinities, both the G10A and G15A forms of ApB had neuronal vs cardiac affinity ratios of 130 and 200, respectively, due mainly to their dramatically slowed association rates. Consequently, both toxins preferred binding to cardiac channels 30−40 times more than did the wild-type toxin.

DISCUSSION

ApB and all homologous anemone toxins contain a region termed the Arg-14 loop consisting of residues 8−17 (ApB numbering), which, when analyzed by two-dimensional NMR, have few medium- to long-range constraints. Previous work from our laboratory using recombinant ApB has demonstrated that one residue within this loop (Arg-12) and one immediately adjacent to it (Leu-18) contribute to channel affinity (*15*−*16*). Because Na_V channels undergo continual conformational transitions throughout their functional cycle, we hypothesized that the three glycine residues present within and nearby the flexible Arg-14 loop might contribute to the toxin's ability to maintain affinity throughout the channel cycle. By substituting alanine for each of the three conserved glycines singly and in combination, we demonstrated the importance of Gly-20 for the structural integrity of the toxin and the importance of Gly-10 and Gly-15 for channel affinity and isoform selectivity.

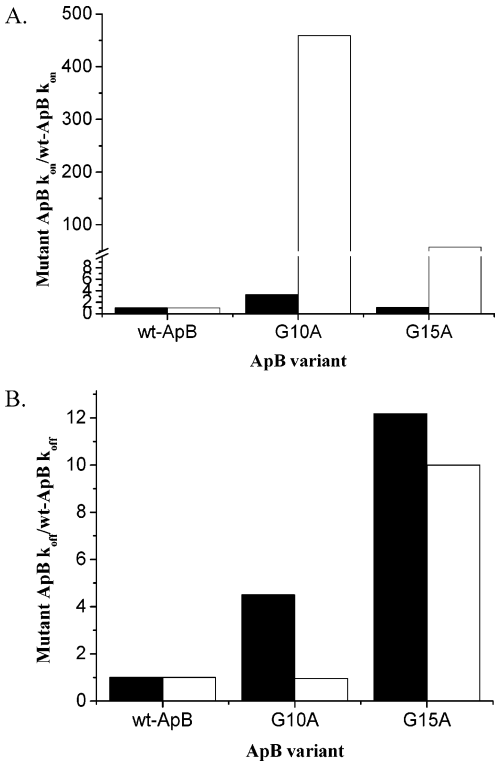

FIGURE 5: Comparison of isoform-specific changes in on- and off-rates of mutant ApB. The upper panel depicts modification rates, and the lower unmodification. The primary data are derived from Table 1. Filled bars are for $Na_V1.5$, and open bars represent $Na_V1.2$.

Although molecular modeling suggested that ApB could accommodate the G20A substitution, consistently poor yields of the G20A protein in combination with its altered CD spectrum led us to conclude that Gly-20 is a folding determinant for ApB. While Gly-20 is in close proximity to the C-terminal end of the Arg-14 loop, it is not part of the loop per se, and its mobility is therefore more limited than that of Gly-10 or Gly-15. Most likely, the constraints imposed on Gly-20 by its presence at the N-terminus of the second β-strand (*10*−*11*) preclude the existence of a side chain at this position. The inability of this mutant toxin to form the necessary β-strand contacts would thus prevent it from folding appropriately.

The G10A, G15A, and G10A/G15A mutant toxins demonstrated CD spectra comparable to that of wt-ApB and are not considered structural determinants. Therefore, these proteins were analyzed by whole cell voltage clamp to determine the functional role of the Gly-10 and Gly-15 residues. The most noticeable alteration in kinetic constants (Figure 5) for the G10A and G15A mutant toxins is in their on-rates to $Na_V1.2$, which are decreased 460- and 60-fold, respectively. In contrast, both toxins associated with $Na_V1.5$ at near wild-type rates. This large isoform discrepancy in k_{on} is reflected in the equilibrium dissociation constants. Thus, when K_D values for $Na_V1.2$ and $Na_V1.5$ are compared, a large isoform discrimination index against $Na_V1.2$ is found. While wt-ApB has an approximately 5-fold preference for $Na_V1.5$, G10A and G15A display 30−40-fold higher discrimination indices despite their overall lower K_D values for both channels. On the basis of these results, we conclude that the $Na_V1.5$ and $Na_V1.2$ sites 3 accommodate toxin binding differently, such that Arg-14 loop flexibility is more important to initial toxin association in the latter system. It is possible that local structure changes attendant upon independent G10A and G15A replacements are responsible for the observed functional changes. However, we consider this less likely, because the measured Cα−Cα distances between G10 and G15 in each of the 20 ApB structures reported by Monks et al. (*10*) are so large, ranging from 6.3 to 13.6 Å, with an average distance of 10.7 Å. That the insertion of a methyl group at either position would result in a qualitatively similar phenotypic change seems less likely, therefore, than restriction of flexibility, which is a known consequence of G → A changes.

Many examples of state-dependent toxin binding to voltage-sensitive cation channels are known (*25*−*27*), and it has long been postulated that the inactivated Na_V channel or state has a lower affinity for all site 3 toxins (*5*, *28*) compared to the closed and open conformations. The lower affinity for the inactivated state is reflected in dramatic voltage-dependent acceleration of the dissociation rate constant of the toxins. Interestingly, sea anemone toxins demonstrate less bias against inactivated states than do the more highly structured α-scorpion toxins (*28*). We propose that the ability of anemone toxins to maintain better binding to the inactivated channel than do α-scorpion toxins may be due in part to the flexible Arg-14 loop and its ability to undergo conformational transitions in concert with the channel. Thus, by successfully restricting loop flexibility via alanine substitution for glycines within the loop, we would expect to observe an increase in dissociation rates of the mutant toxins compared to wt-ApB. All complexes studied are, in fact, destabilized relative to the wild type. This suggests a critical role for flexibility of the Arg-14 loop in maintaining high affinity as the channel conformation changes.

Because the increases in k_{off} for G10A are not as large as for G15A, and because larger decreases in k_{on} are found for G10A vs G15A, we conclude that there are differences in the effects of these two mutant toxins. While G10A toxin must overcome a higher energy barrier to bind $Na_V1.2$, its stability once binding has occurred is akin to that of wt-ApB. G15A is a better binder than G10A, but is unable to make new interactions or to maintain existing ones during the channel's conformational cycling and thus dissociates more readily. The solution structures of all type I anemone toxins display a high degree of disorder for residues 8−17 (ApB numbering). Nonetheless, structure−function analyses of the Arg-14 loop region of anthopleurin A (ApA; *11*, *13*) raise the possibility of the existence of limited structure in a portion of the loop. Within the context of a cyclized synthetic peptide, whose sequence includes residues 6−21 of this toxin, Norton and colleagues suggested the existence of a backbone hydrogen bond between Gly-10 and Asn-16. Although no analogous interactions between other loop residues were observed, and while the synthetic peptide studied lacked both channel binding and cardiostimulatory activity, these data suggest that at least a transitory structure may exist in this region. Evidence for transient hydrogen bonds between nonsequential loop residues in both ApA and ApB has also been presented (*10*, *11*), leading to the suggestion that Gly-10 might act as a hinge for the N-terminal portion of the Arg-14 loop. In contrast, Gly-15 exhibits no constraints in any anemone toxin structure and exists in the region of largest flexibility within the loop,

consistent with an important role for a small, freely mobile residue at this position. The predictions made by these structural models suggest that the glycine residues at these positions are important for toxin activity, although for different reasons. Our results showing significantly decreased K_D values for G10A and G15A caused by different kinetic alterations are in agreement with these predictions.

In conclusion, Gly-10 and Gly-15 of ApB toxin are essential for normal site 3 affinity. We postulate that these residues exert their effects by contributing to an increased flexibility of the Arg-14 loop. This in turn permits ApB to maintain tight binding interactions with multiple channel conformational states, albeit to different degrees. The importance of loop flexibility to toxin affinity is also highly dependent on the channel isoform. Because affinity to $Na_V1.2$ is so much lower for G10A and G15A vs wild-type toxin, specifically due to decreased association rates, $Na_V1.2$ binding site 3 must be more restricted than in $Na_V1.5$. The basis for the apparent inability of G20A toxin to fold remains a subject for future study.

ACKNOWLEDGMENT

We thank Dana McLymond for his assistance with protein purification, Connie Mlecko for her assistance with cell culture maintenance, Megan McNulty, Dr. Tom Suchyna, and Dr. Sergio Elenes for their guidance with the Buffalo electrophysiology setup, and Dr. Tony Auerbach for the use of his pipet puller and polisher.

REFERENCES

1. Blumenthal, K. M., and Seibert, A. L. (2003) Voltage-gated sodium channel toxins: poisons, probes and future promise, *Cell. Biochem. Biophys. 32*, 215−238.
2. Cestele, S., and Catterall, W. A. (2000) Molecular mechanisms of neurotoxin action on voltage-gated sodium channels, *Biochimie 82*, 883−92.
3. Catterall, W. A. (1992) Cellular and molecular biology of voltage-gated sodium channels, *Physiol. Rev. 72*, S15−S47.
4. Catterall, W. A. (1988) Structure and function of voltage-sensitive ion channels, *Science 242*, 50−61.
5. Catterall, W. A., and Beress, L. (1978) Sea anemone toxin and scorpion toxin share a common receptor site associated with the action potential sodium ionophore, *J. Biol. Chem. 253*, 7393−7396.
6. Hanck, D. A., and Sheets, M. F. (1995) Modification of inactivation in cardiac sodium channels: Ionic current studies with Anthopleurin-A toxin, *J. Gen. Physiol. 106*, 601−616.
7. Sheets, M. F., and Hanck, D. A. (1999) Gating of skeletal and cardiac muscle sodium channels in mammalian cells, *J. Physiol. 514*, 425−436.
8. Norton, R. S. (1991) Structure and structure−function relationships of sea anemone proteins that interact with the sodium channel, *Toxicon 29*, 1051−1084.
9. Landon, C., Sodano, P., Cornet, B., Bonmatin, J. M., Kopeyan, C., Rochat, H., Vovelle, F., and Ptak, M. (1997) Refined solution structure of the anti-mammal and anti-insect LqqIII scorpion toxin: comparison with other scorpion toxins, *Proteins 28*, 360−374.
10. Monks, S. A., Pallaghy, P. K., Scanlon, M. J., and Norton, R. S. (1995) Solution structure of the cardiostimulant polypeptide Anthopleurin-B and comparison with Anthopleurin-A, *Structure 3*, 791−803.
11. Pallaghy, P. K., Scanlon, M. J., Monks, S. A., and Norton, R. S. (1995) Three-dimensional structure in solution of the polypeptide cardiac stimulant Anthopleurin-A, *Biochemistry 34*, 3782−3794.
12. Fogh, R. H., Kem, W. R., and Norton, R. S. (1990) Solution structure of Neurotoxin I from the sea anemone *Stichodactyla helianthus*, *J. Biol. Chem. 265*, 13016−13028.
13. Gould, A. R., Mabbutt, B. C., Llewellyn, L. E., Goss, N. H., and Norton, R. S. (1992) Linear and cyclic peptide analogues of the polypeptide cardiac stimulant, Anthopleurin-A: 1H-NMR and biological activity studies, *Eur. J. Biochem. 206*, 641−51.
14. Gallagher, M. J., and Blumenthal, K. M. (1992) Cloning and expression of wild-type and mutant forms of the cardiotonic polypeptide Anthopleurin B, *J. Biol. Chem. 267*, 13958−13963.
15. Gallagher, M. J., and Blumenthal, K. M. (1994) Importance of the unique cationic residues Arginine 12 and Lysine 49 in the activity of the cardiotonic polypeptide Anthopleurin B, *J. Biol. Chem. 269*, 254−259.
16. Dias-Kadambi, B. L., Combs, K. A., Drum, C. L., Hanck, D. A., and Blumenthal, K. M. (1996) Leucine 18, a hydrophobic residue essential for high affinity binding of Anthopleurin B to the voltage-sensitive sodium channel, *J. Biol. Chem. 271*, 23828−23835.
17. Khera, P. K., Benzinger, G. R., Lipkind, G., Drum, C. L., Hanck, D. A., and Blumenthal, K. M. (1995) Multiple cationic residues of Anthopleurin B that determine high affinity channel and isoform discrimination, *Biochemistry 34*, 8522−8541.
18. Benzinger, G. R., Kyle, J. W., Blumenthal, K. M., and Hanck, D. A. (1998) A specific interaction between the cardiac sodium channel and site-3 toxin Anthopleruin B, *J. Biol. Chem. 273*, 80−84.
19. Rogers, J. C., Qu, Y., Tanada, N., Scheuer, T., and Catterall, W. A. (1996) Molecular determinants of high affinity binding of α-scorpion toxin and sea anemone toxin in the S3−S4 extracellular loop in domain IV of the sodium channel α subunit, *J. Biol. Chem. 271*, 15950−15962.
20. Hirsch, J. K., and Quandt, F. N. (1996) Down-regulation of Na channel expression by A23187 in N1E-115 neuroblastoma cells, *Brain Res. 706*, 343−46.
21. Benzinger, G. R., Tonkovich, G. S., and Hanck, D. A. (1999) Augmentation of recovery from inactivation by site-3 Na channel toxins: A single-channel and whole-cell study of persistent currents, *J. Gen. Physiol. 113*, 333−346.
22. Kelso, G. J., Drum, C. L., Hanck, D. A., and Blumenthal, K. M. (1996) Role of Pro-13 in directing high-affinity binding of Anthopleurin B to the voltage-sensitive sodium channel, *Biochemistry 25*, 14157−14164.
23. Maggio, F., and King, G. F. (2002) Scanning mutagenesis of a Janus-faced atracotoxin reveals a bipartite surface patch that is essential for neurotoxic function, *J. Biol. Chem. 277*, 22806−13.
24. Sun, Y. M., Bosmans, F., Zhu, R. H., Goudet, C., Xiong, Y. M., Tytgat, J., and Wang, D. C. (2003) Importance of the conserved aromatic residues in the scorpion α-like toxin BmK M1, *J. Biol. Chem. 278*, 24125−24131.
25. Swartz, K., and MacKinnon, R. (1997) Hanatoxin modifies the gating of a voltage-dependent K+ channel through multiple binding sites, *Neuron 18*, 665−73.
26. Swartz, K., and MacKinnon, R. (1997) Mapping the Receptor Site for Hanatoxin, a Gating Modifier of Voltage-Dependent K+ Channels, *Neuron 18*, 675−82.
27. Jiang, Y., Ruta, V., Chen, J., Lee, A., and MacKinnon, R. (2003) The principle of gating charge movement in a voltage-dependent K+ channel, *Nature 423*, 42−48.
28. Gilles, N., Leipold, E., Chen, H., Heinemann, S. H., and Gordon, D. (2001) Effect of depolarization on binding kinetics of scorpion α-toxin highlights conformational changes of rat brain sodium channels, *Biochemistry 40*, 14576−84.

BI035291D